Human 3′-Phosphoadenosine 5′-Phosphosulfate Synthetase (Isoform 1, Brain): Kinetic Properties of the Adenosine Triphosphate Sulfurylase and Adenosine 5′-Phosphosulfate Kinase Domains†

Eric B. Lansdon,‡ Andrew J. Fisher,‡,§ and Irwin H. Segel*,§

Department of Chemistry and Section of Molecular and Cellular Biology, University of California, One Shields Avenue, Davis, California 95616

Received January 23, 2004; Revised Manuscript Received February 12, 2004

ABSTRACT: Recombinant human 3′-phosphoadenosine 5′-phosphosulfate (PAPS) synthetase, isoform 1 (brain), was purified to near-homogeneity from an *Escherichia coli* expression system and kinetically characterized. The native enzyme, a dimer with each 71 kDa subunit containing an adenosine triphosphate (ATP) sulfurylase and an adenosine 5′-phosphosulfate (APS) kinase domain, catalyzes the overall formation of PAPS from ATP and inorganic sulfate. The protein is active as isolated, but activity is enhanced by treatment with dithiothreitol. APS kinase activity displayed the characteristic substrate inhibition by APS (K_I of 47.9 μM at saturating MgATP). The maximum attainable activity of 0.12 μmol min^{-1} (mg of protein)$^{-1}$ was observed at an APS concentration ([APS]$_{opt}$) of 15 μM. The theoretical K_m for APS (at saturating MgATP) and the K_m for MgATP (at [APS]$_{opt}$) were 4.2 μM and 0.14 mM, respectively. At likely cellular levels of MgATP (2.5 mM) and sulfate (0.4 mM), the overall endogenous rate of PAPS formation under optimum assay conditions was 0.09 μmol min^{-1} (mg of protein)$^{-1}$. Upon addition of pure *Penicillium chrysogenum* APS kinase in excess, the overall rate increased to 0.47 μmol min^{-1} (mg of protein)$^{-1}$. The kinetic constants of the ATP sulfurylase domain were as follows: $V_{max,f} = 0.77$ μmol min^{-1} (mg of protein)$^{-1}$, $K_{mA(MgATP)} = 0.15$ mM, $K_{ia(MgATP)} = 1$ mM, $K_{mB(sulfate)} = 0.16$ mM, $V_{max,r} = 18.7$ μmol min^{-1} (mg of protein)$^{-1}$, $K_{mQ(APS)} = 4.8$ μM, $K_{iq(APS)} = 18$ nM, and $K_{mP(PPi)} = 34.6$ μM. The (a) imbalance between ATP sulfurylase and APS kinase activities, (b) accumulation of APS in solution during the overall reaction, (c) rate acceleration provided by exogenous APS kinase, and (d) availablity of both active sites to exogenous APS all argue against APS channeling. Molybdate, selenate, chromate ("chromium VI"), arsenate, tungstate, chlorate, and perchlorate bind to the ATP sulfurylase domain, with the first five serving as alternative substrates that promote the decomposition of ATP to AMP and PP_i. Selenate, chromate, and arsenate produce transient APX intermediates that are sufficiently long-lived to be captured and 3′-phosphorylated by APS kinase. (The putative PAPX products decompose to adenosine 3′,5′-diphosphate and the original oxyanion.) Chlorate and perchlorate form dead-end E·MgATP·oxyanion complexes. Phenylalanine, reported to be an inhibitor of brain ATP sulfurylase, was without effect on PAPS synthetase isoform 1.

ATP sulfurylase (ATP:sulfate adenylyltransferase, EC 2.7.7.4) and APS[1] kinase (MgATP:adenylyl sulfate, EC 2.7.1.25) catalyze, in order, the two-step activation of inorganic sulfate to form first adenosine 5′ phosphosulfate (adenylyl sulfate, APS) and then 3′-phosphoadenosine 5-phosphosulfate (3′-phosphoadenylyl sulfate, PAPS):

$$MgATP + SO_4^{2-} \rightleftharpoons MgPP_i + APS \text{ (ATP sulfurylase)}$$

$$MgATP + APS \rightleftharpoons MgADP + PAPS \text{ (APS kinase)}$$

In many heterotrophic bacteria, yeasts, fungi, algae, and higher plants, either PAPS or APS enters into a reductive assimilation pathways that leads to cysteine and ultimately, to all the reduced sulfur-containing biomolecules. PAPS also serves as the sulfuryl donor for the biosynthesis of sulfate esters in all types of cells (*1*). For example, animal tissues produce cerebroside sulfate (sulfolipid) in nervous tissue,

† The research described in this report was initiated with support from NSF Research Grant MCB 9904003 to I.H.S. and A.J.F. and by facilities of the W. M. Keck Foundation Center for Structural Biology at the University of California, Davis. E.B.L. is supported by the University of California System-Wide Biotechnology Research Program, Grant 2001-07.

* Corresponding author: e-mail ihsegel@ucdavis.edu; phone 530-752-3193; fax 530-752-3085.

‡ Department of Chemistry.

§ Section of Molecular and Cellular Biology.

[1] Abbreviations: APS, adenosine 5′-phosphosulfate (adenylyl sulfate); PAPS, 3′-phosphoadenosine 5′-phosphosulfate (adenylyl sulfate 3′-phosphate); AMP, ADP, and ATP, adenosine mono-, di-, and triphosphate; Ap_5A, diadenosine pentaphosphate; APX and PAPX, putative 5′-nucleotide product of a divalent oxyanion other than sulfate and its putative 3′-phospho derivative; PAP, adenosine 3′,5′-diphosphate; MgATP, MgADP, and $MgPP_i$, magnesium complexes with the associated nucleotides; DTT, dithiothreitol; EDTA, ethylenediaminetetraacetic acid; IPTG, isopropyl β-D-thiogalactoside; NADH, nicotinamide adenine dinucleotide, reduced form; $NADP^+$, nicotinamide adenine dinucleotide phosphate, oxidized form; PAPSS, 3′-phosphoadenosine 5′-phosphosulfate synthetase; PCR, polymerase chain reaction; PEP, phosphoenol pyruvate; PP_iase, inorganic pyrophosphatase; Tris, tris(hydroxymethyl)aminomethane.

10.1021/bi049827m CCC: $27.50
Published on Web 03/17/2004

sulfated cell surface oligosaccharides, sterol and steroid sulfates, and chondroitin sulfate. Sulfation is a common modification of many secreted signal biomolecules, e.g., neuropeptides, catecholamines, coagulation factors, and heparan sulfates. The last bind to growth factors, receptors, cell adhesion molecules, etc., to regulate cell proliferation and differentiation (*2*, *3*). Tyrosine sulfation is a posttranslational modification of many secreted proteins and has been shown to play a critical role in the function of the human immunodeficiency virus type 1 (HIV-1) coreceptor (*4*, *5*). PAPS-dependent sulfation has long been recognized as an important route for the detoxification of phenolic xenobiotics (e.g., acetaminophen) and endogenous bile acids (glycolithocholate) (*6*), and for the activation of some carcinogens (*7*).

The two sulfate-activating enzymes are separate proteins in most bacteria, yeast, fungi, algae, and higher plants. But in animal tissues, the two activities are co-located on a single polypeptide chain—a feature first proposed by Schwartz and co-workers (*8*) and later confirmed when the gene was identified (*9*, *10*). Residues 1−ca. 231 comprise APS kinase (*11*, *12*); residues ca. 394−624 correspond to the catalytic domain of ATP sulfurylase (*13*−*16*). The intervening region (residues 232−393) is analogous to the N-terminal domain of monofunctional ATP sulfurylases. Three normal isoforms of this "PAPS synthetase" protein have been described: PAPSS1 is the major form in brain and skin. PAPSS2 predominates in liver and cartilage. A splice variant of PAPSS2 (called PAPSS2b) that contains five extra amino acid residues (GMALP) in the N-terminal region has also been identified. PAPS1 is targeted to the nucleus of mammalian cells (*17*); PAPSS2 is cytosolic. Mutations in PAPSS2 are associated with severe connective tissue abnormalities as seen in human spondyloepimetaphyseal dysplasia (*18*) and mouse brachyomorphism (*19*).

Recent research has provided much information about the genetics, tissue expression, domain organization, and essential residues of PAPS synthetase. But there are still unanswered questions about the functional properties of the enzyme. In this report, we examine the kinetic characteristics of the individual sulfurylase and kinase activities of PAPSS1 and the assumption of APS channeling (*20*−*22*).

EXPERIMENTAL PROCEDURES

Cloning. Human PAPS synthetase isoform 1 (GenBank Accession Number O43252) was cloned from human fetal brain cDNA (Invitrogen). PCR primers were as follows: upstream, 5′-GTGCCTCATATGGAGATCCCCGGGAGCTTG-3′; downstream, 5′-GCTCGAGTGCGGCCGCAGCTTTCTC-CAAGGATTTG-3′. Restriction sites designed for *Nde*I in the upstream primer and for *Not*I in the downstream primer are underlined. After PCR the product was subcloned into pET22b(+) vector (Novagen).

Protein Expression and Purification. Human PAPSS synthetase I was chemically transformed into *E. coli* strain BL21 (DE3) Gold (Stratagene) and overexpressed. Typically, 3-L cultures were grown to an A_{600} of 0.6 at 37 °C. Cultures were then cooled to 15 °C and induced with 0.5 mM IPTG for 15−17 h. The cells were centrifuged and then resuspended in 50 mM sodium/potassium phosphate, pH 8.0, containing 0.5 M NaCl and 10 mM imidazole free base. The suspension was passed through a Microfluidizer (model M-110Y) several times to break the cells. Insoluble cell debris was then removed by centrifugation. The resulting lysate was passed through a Ni−nitrilotriacetate (NTA) resin (Qiagen) previously charged with nickel sulfate and washed with the above buffer until the A_{280} was less than 0.05. Protein was then eluted with the above buffer containing 20 mM imidazole. The eluate was dialyzed against 50 mM sodium/potassium phosphate, pH 8.0, containing 50 mM NaCl and 1 mM EDTA. (This buffer was used for all remaining purification steps.) The solution was then applied to a Matrix Green A (Amicon) column, previously found to be useful for purification of the rat liver enzyme (*23*). Protein was eluted with a 0−3 M NaCl gradient in the above phosphate buffer. The final step was anion exchange on Q-Sepharose. Protein was eluted with a 0−0.5 M NaCl gradient in the above phosphate buffer. The final preparation, judged to be greater than 95% pure by sodium dodecyl sulfate−polyacrylamide gel electrophoresis (SDS−PAGE), was dialyzed against and stored in 20 mM sodium/potassium phosphate, pH 8.0, containing 100 mM NaCl, 5% glycerol, and 1 mM EDTA.

Chemicals and Coupling Enzymes. ATP, NADH, $NADP^+$, PEP, and other assay components were purchased from Sigma as listed earlier (*24*). Coupling enzymes were also obtained from Sigma, except for recombinant *Penicillium chrysogenum* APS kinase, which was purified as described earlier (*25*).

Enzyme Assays. ATP sulfurylase activities were measured by continuous coupled spectrophotometric assays (*26*, *27*, *24*). All assays were conducted at 30 °C in Tris-HCl buffer, pH 8.0. In the forward (APS synthesis) direction, activity was coupled to excess APS kinase, pyruvate kinase, and lactate dehydrogenase in the presence of excess inorganic pyrophosphatase and, in some assays, 5 mM DTT. This assay quantifies the rate of ADP formation. In some experiments APS kinase and/or PP_iase were omitted to duplicate the assay conditions used in other reports. The reaction was started by adding sulfate or the purified PAPSS1. Activity with molybdate or another reactive divalent oxyanion was measured by substituting the oxyanion for sulfate and, in some cases, myokinase (adenylate kinase) for APS kinase. The myokinase-coupled assay quantifies the rate of AMP formation. The reverse (ATP synthesis) reaction was assayed by coupling the formation of ATP to hexokinase and glucose-6-phosphate dehydrogenase in the presence of 1 mM glucose, 0.3 mM $NADP^+$, and 5 mM $MgCl_2$. When one substrate was varied, the other was present at a saturating concentration. The reaction was started by adding APS and PP_i simultaneously.

K_{iq} for APS binding to the ATP sulfurylase domain was determined by measuring the inhibition of the molybdolysis reaction by APS. The reaction was started by adding MoO_4^{2-} and APS simultaneously (to minimize APS depletion by the APS kinase domain), and the rate was measured as soon as the ΔA_{340} became constant. (There is an initial activity burst because commercial APS contains a small amount of AMP as a breakdown product.)

APS kinase activity was measured by continuously monitoring the rate of ADP formation (as described above) in the presence of excess nuclease P1, 1 mM $NaClO_3$, and

50 μM Ap_5A. Nuclease P1 maintains APS at a constant level throughout the assay by removing the 3′-phospho group as rapidly as it is added. Chlorate inhibits the ATP sulfurylase activity minimizing loss of APS by a reaction with contaminating PP_i in the ATP. Ap_5A was included to inhibit myokinase that was present as a trace contaminant in the pyruvate kinase + lactate dehydrogenase mixture. For these assays, the enzyme was preincubated with 5 mM DTT for 15 min. (DTT could not be included in the assay mixture because it inactivates nuclease P1.) Enzyme concentrations were usually between 5 and 30 μg/mL in kinetics studies. These levels yielded a ΔA_{340} that was between 0.02 and 0.03 min^{-1} as measured on a Perkin-Elmer Lambda model 11 or a Gilford model 250 spectrophotometer.

The presence of PAP in APS kinase-coupled assay mixtures with selenate, arsenate, or chromate as the inorganic substrate was confirmed by the following procedure: At the end of the incubation period, ATP sulfurylase (along with the other enzymes) was removed by centrifugation through a 30 kDa cutoff membrane filter (Millipore Ultrafree-MC). Myokinase, pyruvate kinase, and lactate dehydrogenase were then added back and the ΔA_{340} was measured after the reaction was started by adding 10 units of nuclease P1.

Data Analyses. v vs [APS] data for APS kinase were fitted to the equation for substrate inhibition (*28*):

$$v = \frac{V_{max}[APS]}{K_{mQ} + [APS] + \frac{[APS]^2}{K_{IQ}}} \quad (1)$$

where V_{max}, K_{mQ}, and K_{IQ} are apparent constants for APS at the fixed [MgATP]. The last is the inhibition constant for APS binding to E·MgADP to form a dead-end E·APS·MgADP complex.

The v vs [MgATP] at $[APS]_{opt}$ and all velocity curves for ATP sulfurylase were fitted to the Henri−Michaelis−Menten equation:

$$v = \frac{V_{max,app}[S]}{K_{m,app} + [S]} \quad (2)$$

where $V_{max,app}$ and $K_{m,app}$ are the apparent constants for the varied substrate at the fixed concentration of the cosubstrate. $V_{max,app}$ values were replotted against the cosubstrate concentration to obtain the limiting V_{max} and the K_m of the cosubstrate. The data were also analyzed by double-reciprocal plots and appropriate replots (*29*).

K_{iq} for the inhibition of ATP sulfurylase by APS was calculated from $[APS]_{0.5}$, the concentration of APS that yielded 50% inhibition at known levels of MgATP and molybdate. The original plot of relative activity, v_i/v_0, vs [APS] was fitted to

$$\frac{v_i}{v_0} = Z - \frac{M[APS]}{[APS]_{0.5} + [APS]} \quad (3)$$

where Z is the starting value of v_i/v_0 and M is the maximum degree of inhibition. (Both of these values should be 1.0 if the curve fits well and the inhibitor can drive the velocity to zero.) Then K_{iq} was calculated from

$$K_{iq} = \frac{[APS]_{0.5}}{1 + \frac{[MgATP]}{K_{ia}} + \frac{[MoO_4^{2-}]}{K_{ib}} + \frac{[MgATP][MoO_4^{2-}]}{K_{ia}K_{mB}}} \quad (4)$$

The K_{eq} of the ATP sulfurylase reaction was calculated from the Haldane equation:

$$K_{eq} = \frac{V_{max,f}K_{i(APS)}K_{m(PPi)}}{V_{max,r}K_{i(MgATP)}K_{m(sulfate)}} \quad (5)$$

For simulation studies, the equilibrium concentration of APS was first calculated from

$$[APS]_{eq} = \sqrt{K_{eq}[MgATP][SO_4^{2-}]} \quad (6)$$

Then the APS kinase rate at $[APS]_{eq}$ was calculated from eq 1 and plotted against the original [MgATP]. The simulated v vs [MgATP] plot was fitted to eq 2 and to the Hill equation:

$$v = \frac{V_{max}[MgATP]^{n_H}}{K' + [MgATP]^{n_H}} \quad (7)$$

where n_H is the Hill coefficient and K' is equivalent to $[MgATP_{0.5}]^{n_H}$.

All curve fits were performed with DeltaGraph Pro 4.05 c (Macintosh). Fits to primary velocity curves (e.g., Figures 1, 2, and 4) generally had an R^2 value of >0.99. The maximum error in kinetic constants obtained from replicate plots was usually less than ±15% of the mean.

The level of contaminating sulfate in a nonsulfate inorganic ligand that would be required to yield the observed APS kinase-coupled activity (assuming that all of the activity resulted from the sulfate) was calculated from the relationship presented in (*23*)

$$\frac{V_{maxC,app}}{K_{mC,app}} = \frac{nrV_{maxB,app}}{K_{mB,app}} \quad (8)$$

where $V_{maxC,app}$ and $K_{mC,app}$ are the apparent kinetic constants of the nonsulfate inorganic compound provided as the substrate (compound C), $V_{maxB,app}$ and $K_{mB,app}$ are the apparent kinetic constants for sulfate under the same assay conditions, r is the ratio of molecular weights of the substrates (MW_C/MW_B), and n is the fractional weight contamination of compound C by sulfate (e.g., Na_2SO_4 present in the Na_2HPO_4).

RESULTS AND CONCLUSIONS

Native Molecular Weight. Purified PAPSS1 eluted from a calibrated Toyopearl HW-55 column at a position very close to that of alchohol dehydrogenase (ca. 150 kDa). The theoretical subunit molecular mass (including His_5 plus the linker) is 72 kDa, so it appears that the native enzyme is a dimer, as reported earlier for the enzyme purified from rat liver (*23*).

APS Kinase Activity. Figure 1 shows the velocity curves of the APS kinase activity of PAPSS1 at low and high salt and high salt plus DTT. The profiles are qualitatively similar

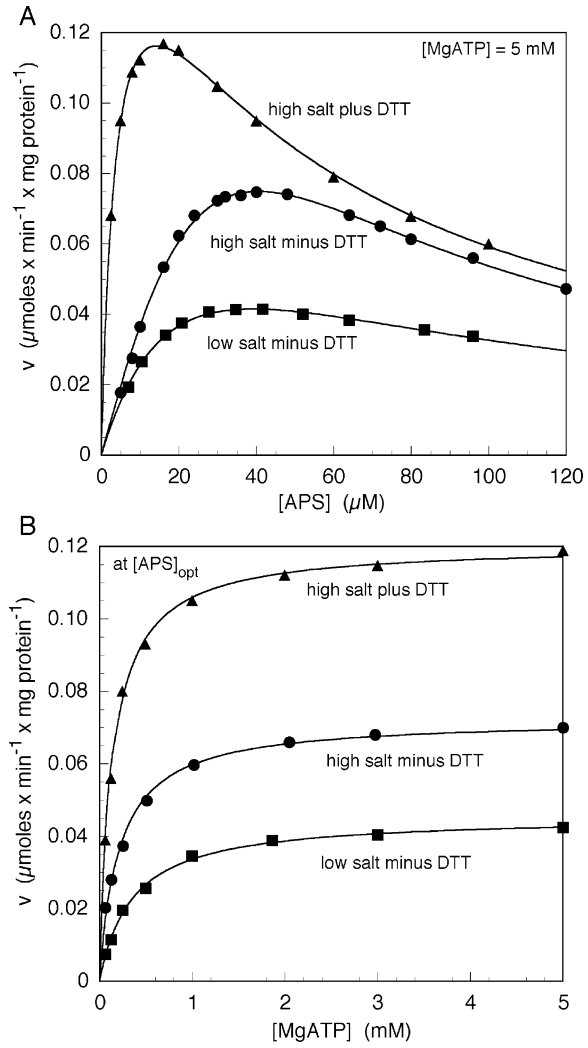

FIGURE 1: Kinetics of the APS kinase activity of human PAPSS1. Low-salt assays were conducted in the standard reaction mixture (50 mM Tris-HCl buffer plus other components listed under Materials and Methods). High-salt assays were conducted in the same reaction mixture to which 100 mM NaCl was added. For the plus DTT assays, the stock enzyme solution was preincubated with 5 mM DTT for 15 min prior to the assay. (A) v vs [APS] at 5 mM MgATP. The kinetic constants obtained by fitting the curve to eq 1 were as follows: $V_{max,theor} = 0.19$ μmol min^{-1} (mg of protein)$^{-1}$, $K_{m(APS)} = 4.2$ μM, and $K_{IB} = 47.9$ μM. (B) v vs [MgATP] at $[APS]_{opt}$ (15 μM). The kinetic constants obtained by fitting the data to eq 2, where $V_{max,app} = 0.12$ μmol min^{-1} (mg of protein)$^{-1}$ and $K_{mA,app} = 0.14$ mM.

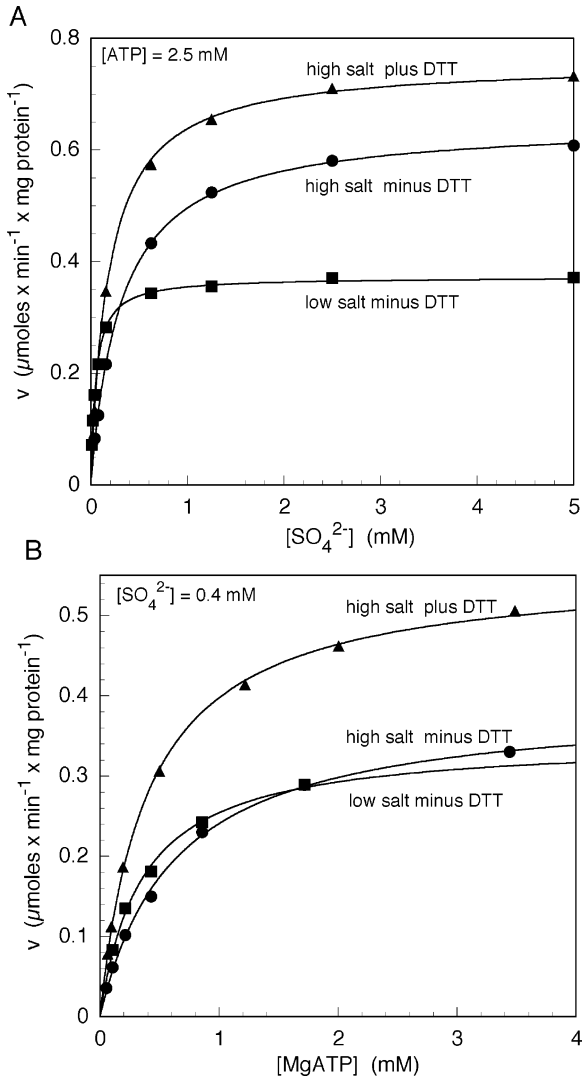

FIGURE 2: Kinetics of the ATP sulfurylase activity of human PAPSS1. Each curve was fitted to eq 2 to yield a $K_{m,app}$ and $V_{max,app}$ at the fixed subsaturating cosubstrate concentration. DTT, when present, was 5 mM in the assay mixture. (A) v vs $[SO_4^{2-}]$ at 2.5 mM MgATP. Under optimum conditions, $V_{max,app} = 0.76$ μmol min^{-1} (mg of protein)$^{-1}$ and $K_{mB,app} = 0.19$ mM. (B) v vs [MgATP] at 0.4 mM SO_4^{2-}. Under optimum conditions, $V_{max,app} = 0.55$ μmol min^{-1} (mg of protein)$^{-1}$and $K_{mA.app} = 0.40$ mM. The limiting kinetic constants are listed in Table 1.

to those of APS kinases from several other sources (*25*, *30*, *31*) in that (a) APS displays substrate inhibition but (b) the v vs [MgATP] plot is hyperbolic. Also (c) high salt "activates" the enzyme. But compared to other APS kinases, the v vs [APS] profile of PAPSS1 is shifted to a higher substrate concentration and the activity of the enzyme (either the theoretical k_{cat} or the v at optimum [APS]) is quite a bit lower. DTT activated PAPSS1 beyond that provided by the increased ionic strength. This was not unexpected considering that human PAPSS1 contains 14 Cys residues, of which eight are within the APS kinase domain. (Some disulfide linkages may have formed accidentally during purification.) Under optimum conditions, K_{mB} (the Michaelis constant for APS) and K_{IB} (the substrate inhibition constant) were 4.2 μM and 47.9 μM, respectively. The theoretical V_{max} is about 0.19 μmol min^{-1} (mg of protein)$^{-1}$. But because of the substrate inhibition, the maximal velocity attainable (v_{opt}) is 0.12 μmol min^{-1} (mg of protein)$^{-1}$ at the $[APS]_{opt}$ of 15 μM. An earlier study of the kinetics of purified human brain PAPSS conducted over a lower [APS] range did not detect substrate inhibition (*32*).

ATP Sulfurylase Activity (APS Synthesis Direction). The ATP sulfurylase reaction catalyzed by PAPSS1 was assayed in the presence of yeast PP_iase and *P. chrysogenum* APS kinase, both added in large excess. If APS dissociates from the sulfurylase active site before rebinding to the kinase site, the kinetic constants obtained from this rate data would correspond to those of the ATP sulfurylase activity. If APS did not dissociate (but rather was channeled directly to the APS kinase domain), the added APS kinase would have no effect on the assay, while the added PP_iase might still be beneficial by removing a potential product inhibitor. Figure 2 shows initial velocity plots for a cosubstrate concentration that was fixed at a likely in vivo level. These were 2.5 mM

Table 1: Kinetic Constants of Human PAPSS 1[a]

constant	ATP sulfurylase	APS kinase
$V_{max,f(sulfate)}$	0.77 unit/mg	0.19 unit/mg[b]
$V_{max,f(molybdate)}$	31.5 units/mg	
$V_{max,r}$	18.7 units/mg	
$K_{mA(MgATP/sulfate)}$	0.15 mM	0.14 mM
$K_{mA(MgATP/molybdate)}$	0.1 mM	
$K_{ia(MgATP/sulfate)}$	1.1 mM	
$K_{ia(MgATP/molybdate)}$	1.0 mM	
$K_{mB(sulfate)}$	0.16 mM	
$K_{mB(molybdate)}$	1.3 mM	
$K_{ib(sulfate)}$	1.7 mM	
$K_{ib(molybdate)}$	14.3 mM	
$K_{mQ(APS)}$	4.8 μM	4.2 μM
$K_{mP(PPi)}$	34.6 μM	
$K_{iq(APS)}$	18 nM	
K_{eq}	1.4×10^{-7}	
$K_{IQ,app(APS)}$		47.9 μM
$[APS]_{opt}$[c]		15 μM
v_{opt}		0.12 unit/mg

[a] All constants were determined in 0.05 M Tris-HCl buffer containing 100 mM NaCl at pH 8.0, 30 °C. ATP sulfurylase assay mixtures contained 5 mM DTT. The enzyme stock solution used for APS kinase assays was pretreated with 5 mM DTT. Subscript A refers to MgATP for both activities. Subscript B refers to sulfate or molybdate in the reaction with ATP sulfurylase. Q refers to APS for both enzymes. P refers to PP_i for ATP sulfurylase. The ATP sulfurylase reaction is believed to follow a random A/B, ordered P/Q kinetic mechanism (*40*). Entries left blank were not applicable or not determined. K_m is the limiting Michaelis constant at saturating cosubstrate (except for the K_{mA} of APS kinase, which was obtained at $[APS]_{opt}$). K_i is the dissociation constant of the indicated binary E·ligand complex. $K_{IQ,app}$ is the apparent APS substrate inhibition constant of APS kinase at 5 mM MgATP. The APS kinase reaction is believed to follow an ordered sequence with MgATP adding before APS, PAPS leaving before MgADP, and APS binding to E·MgADP to form a dead-end EBQ complex (*28*). [b] Theoretical V_{max} from curve fits. This rate cannot be obtained because of substrate inhibition of the APS kinase reaction by APS. [c] $[APS]_{opt}$ is the APS concentration at the peak APS kinase velocity. $[APS]_{opt} = \sqrt{K_{mQ,app}K_{IQ,app}}$, where $K_{mQ,app}$ and $K_{IQ,app}$ are the apparent Michaelis and substrate inhibition constants for APS at the fixed [MgATP].

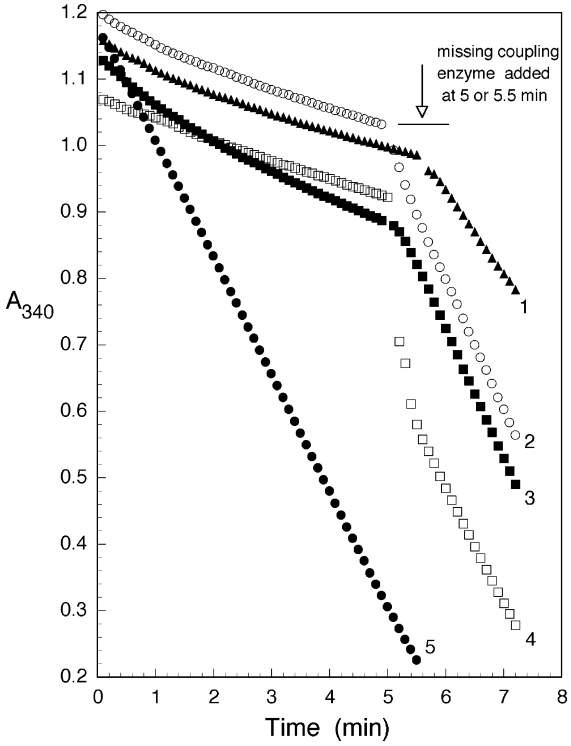

FIGURE 3: Spectrophotometric tracings of the overall PAPS synthesis reaction. The reaction mixtures (each 1.0 mL total volume) contained 2.5 mM MgATP, sulfate as indicated below, 100 mM NaCl, ca. 0.3 mM NADH (varied slightly to yield different starting absorbances), 7.5 mM KCl, 0.8 mM PEP, 5 mM excess $MgCl_2$, 5 mM DTT, 15 units of pyruvate kinase, 25 units of lactate dehydrogenase, and 45 μg of homogeneous PAPSS1 all in 50 mM Tris-HCl, pH 8.0 at 30° C. Pure *P. chrysogenum* APS kinase (6 μg) or 5 units of yeast inorganic pyrophosphatase (whichever was missing) was added at 5 or 5.5 min. Absorbance readings were recorded every 0.1 min. (Curve 1) Initially missing APS kinase at 0.4 mM SO_4^{2-}; (curve 2) initially missing APS kinase at 5 mM SO_4^{2-}; (curve 3) initially missing PP_iase at 5 mM SO_4^{2-}; (curve 4) initially missing APS kinase at 100 mM SO_4^{2-}; (curve 5) complete assay mixture with APS kinase and PP_iase present from zero time at 5 mM SO_4^{2-}.

for MgATP (*33*−*36*) and 0.4 mM for sulfate (*37*−*39*). High salt increased both the V_{max} of the sulfurylase activity and the Michaelis constant for sulfate, the latter to a value in the region of the presumed intracellular level. DTT provided an additional increase in activity. At 2.5 mM MgATP, the Michaelis constant for sulfate ($K_{mB,app}$) was 0.19 mM; at 0.4 mM sulfate, the Michaelis constant for MgATP ($K_{mA,app}$) was 0.4 mM. In separate experiments, v vs [sulfate] and v vs [MgATP] curves were obtained over a wide range of fixed cosubstrate concentrations (data not shown). All plots were hyperbolic within experimental error (i.e., the Hill coefficients were 1.0 ± 0.1). Table 1 summarizes the limiting Michaelis constants of PAPSS1 under optimum conditions.

The above results show that, at in vivo levels of ATP and sulfate, the maximal attainable APS kinase activity of the *E. coli*-expressed PAPSS1 at pH 8.0, 30 °C (ca. 0.12 μmol min^{-1} (mg of protein)$^{-1}$ at $[APS]_{opt}$), is lower than that of the colocated ATP sulfurylase activity [ca. 0.47 μmol min^{-1} (mg of protein)$^{-1}$] under the same conditions. This imbalance can be observed directly in the spectrophotometer tracings (Figure 3). The overall reaction proceeds in the absence of added APS kinase, but the rate (a) slows continuously and (b) is markedly increased upon addition of excess *P. chrysogenum* APS kinase (curves 1, 2, and 4). The results confirm that the endogenous APS kinase activity of PAPSS1 is not sufficient to keep pace with the sulfurylase activity under the assay conditions. The transient decrease in A_{340} observed immediately after addition of the excess APS kinase to the cuvette containing 100 mM sulfate (as shown in Figure 3, curve 4, before the rate becomes constant) corresponds to an accumulated APS pool of about 60 μM. This pool is much larger than that accumulated during the first phase of the assay at lower sulfate concentrations, but it cannot be attributed simply to a difference in substrate availability because the K_m for sulfate is about 0.19 mM under assay conditions. Rather, the increased APS accumulation almost certainly results from the reduction in product inhibition exerted by APS at the elevated sulfate concentration (see below).

Product Inhibition by APS. APS was competitive with both MgATP and molybdate (data not shown). This pattern is consistent with the rapid equilibrium random binding of substrates as reported for ATP sulfurylases from other sources (*40*, *23*, *27*, *41*, *24*). At 5 mM MgATP and 5 mM molybdate, APS inhibited the molybdolysis reaction with an $[I]_{0.5}$ of 0.46 μM (data not shown). Because of the competitive inhibition by the substrates, the limiting K_{iq} is much

Table 2: Effect of Coupling Enzymes on the Overall PAPS Synthesis Rate

incubation mixture	PAPS synthesis rate [μmol min^{-1} (mg of protein^{-1})]		
	low salt	high salt	high salt + DTT
complete[a]	0.30	0.31	0.47
minus APS kinase	0.034	0.05	0.09
minus PP_iase	0.035	0.034	0.14
minus APS kinase and minus PP_iase	0.01	0.01	0.07

[a] The complete reaction mixture contained excess *P. chrysogenum* APS kinase, yeast PP_iase, and the other coupling enzymes as described under Materials and Methods. MgATP was present at 2.5 mM. High-salt assay mixtures contained an additional 100 mM NaCl. DTT (when present) was 5 mM. The PAPSS1 level was 15 μg/mL in the complete mixture and 45 μg/mL in the others. Reactions were started by adding the sulfate to a final concentration of 0.4 mM. Rates were measured over the next 1−3 min.

lower and can be calculated from eq 4 to be 0.46/25.6 = 18 nM. The extremely high affinity of APS for the enzyme would further confound initial velocity measurements in the absence of added APS kinase. On the other hand, PAPS, which is formed in the assay, was much less inhibitory to the ATP sulfurylase activity; 75 μM PAPS produced only 25% inhibition at K_m levels of MgATP and sulfate (data not shown).

Product inhibition of ATP sulfurylase by APS is necessarily studied in the presence of both substrates of the APS kinase reaction. This raises the possibility that some of the observed inhibition might result from a substrate-induced conformational change at the APS kinase active site that is transmitted to the sulfurylase domain. An interaction between the APS kinase-like regulatory domain and the catalytic domain of fungal ATP sulfurylase has been shown to modulate activity in that enzyme even in the absence of the allosteric effector (*42*).

Effect of Inorganic Pyrophosphatase. In most earlier studies of animal PAPSS, PP_iase was not included in the assay mixture. In fact, Lyle et al. (*20*) reported that PP_iase had a slightly negative effect on the overall PAPS synthesis reaction. In our assays, PP_iase was essential, as shown in Figure 3 (curve 3). In the absence of PP_iase, (but with excess APS kinase present), the rate slowed noticeably over the first 2 min, an indication that PP_i, like APS, is a strong inhibitor of ATP sulfurylase. Table 2 summarizes the effects of added coupling enzymes on the overall reaction rate. The cumulative results show clearly that rates obtained in the absence of added APS kinase and PP_iase may not reflect the intrinsic activity of either domain of PAPSS1. The omission of PP_iase may have been of little consequence when the source of the enzyme was an unfractionated cell extract (*43*−*45*) but may have influenced rates when a purified preparation was used (*22*). It should be noted that the major source of PP_i might not be the small amount accumulated in short-term assays but rather the ATP stock solution. Freshly prepared ATP solutions contain about 0.02 mol % PP_i (*46*) and the level probably increases upon storage. PP_i contamination is not a trivial matter when it is considered that ATP is generally used in PAPSS assays at millimolar levels while the K_i for PP_i is generally in the micromolar range (*47*, *41*).

Steady-State Rate. Although the ATP sulfurylase activity of PAPSS1 is higher than the colocated APS kinase activity,

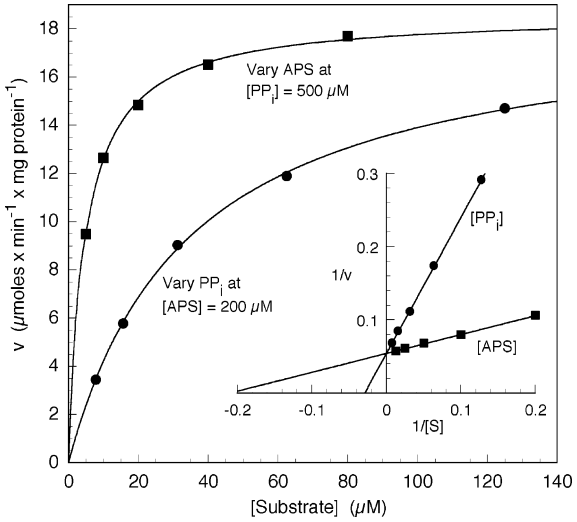

FIGURE 4: Kinetics of the reverse (ATP synthesis) reaction. Each substrate was varied at a saturating concentration of the cosubstrate. (Inset) Double-reciprocal plot of the primary data. The plots yielded $V_{max,r}$ = 18.7 μmol min^{-1} (mg of protein)$^{-1}$, $K_{m(APS)}$ = 4.8 μM, and $K_{m(PPi)}$ = 34.6 μM.

the former is much more sensitive to inhibition by APS. Thus there must be some steady-state level of APS that equalizes the two activities. This level was estimated by setting the velocity equations for the two activities equal to each other (eq 9) at presumed cellular levels of substrates. The values of the kinetic constants were taken from Table 1. V_1 and V_2 are the respective $V_{max,f}$ values of the ATP sulfurylase and APS kinase activities. It was assumed that K_{ia} and K_{mA} are identical for the APS kinase reaction (*48*):

$$\frac{V_1[A][B]}{K_{ia}K_{mB} + K_{mA}[B] + K_{mB}[A] + [A][B] + \dfrac{K_{ia}K_{mB}[Q]}{K_{iq}}} = \frac{V_2[A][Q]}{K_{ia}K_{mQ} + K_{mA}[Q] + K_{mQ}[A] + [A][Q] + \dfrac{[A][Q]^2}{K_{IQ}}} \quad (9)$$

At 2.5 mM MgATP (A) and 0.4 mM sulfate (B), the calculation yields a steady-state APS (Q) concentration of 1.6 μM, which would lead to a velocity of about 0.05 μmol min^{-1} (mg of protein)$^{-1}$. This is in reasonable agreement with the observed "minus APS kinase" assay rate of ca. 0.09 μmol min^{-1} (mg of protein)$^{-1}$ (Table 2) when it is considered that the rate had not yet attained its final level. The calculated rate is also similar to that reported for mouse PAPSS1 [0.04 μmol min^{-1} (mg of protein)$^{-1}$] by Singh and Schwartz (*49*). In vivo, the overall PAPS synthetase activity would be modulated not only by product inhibition of ATP sulfurylase and substrate inhibition of APS kinase by APS but also by PAPS inhibition at both sites.

Kinetics of the Reverse ATP Sulfurylase Reaction. V_{max} for the energetically favorable reverse reaction (ATP synthesis direction) was 18.7 units/mg of protein (Figure 4). Thus the forward and reverse V_{max} values for PAPSS1 (0.77 and 18.7) are similar to those reported for native ATP sulfurylase purified from rat liver (ca. 2 and 20) by Yu et al. (*23*).

Table 3: Reaction of PAPSS1 with Other Divalent Inorganic Oxyanions[a]

inorganic substrate	$K_{mA,app}$ (mM)	$K_{mB,app}$ (mM)	$V_{max,app}$ [μmol min^{-1} (mg of protein^{-1})]	$V_{max,app}/K_{mB,app}$
MoO_4^{2-}	0.49	1.5	27.0	18
WO_4^{2-}	0.60	4.5	26.9	6
CrO_4^{2-}				
APSK-coupled	0.40	0.05	4.2	84
MK-coupled	0.06	0.12	7.0	58
SeO_4^{2-}				
APSK-coupled	0.07	0.35	1.0	2.9
MK-coupled	0.16	0.52	0.93	1.8
$HAsO_4^{2-}$				
APSK-coupled	5.0	1.7	0.08	0.05
MK-coupled	1.8	18.5	1.7	0.09
HPO_4^{2-}				
neither	1.5	2.7	0.08	0.03

[a] Rates with MoO_4^{2-}, WO_4^{2-}, CrO_4^{2-}, SeO_4^{2-}, and $HAsO_4^{2-}$ were measured under high-salt assay conditions. DTT (5 mM) was also present except when CrO_4^{2-} was the substrate. (In this case, the stock enzyme was preincubated with 5 mM DTT before dilution into the assay mixture). APS kinase-coupled reaction mixtures contained 50 μM Ap_5A to suppress the contaminating myokinase activity. Neither APS kinase (which quantifies ADP formation) nor myokinase (which quantifies AMP formation) was added when phosphate was the substrate. (The P_i-dependent reaction would produce ADP directly.) When MgATP was varied, the inorganic substrate was present at 5 mM, except for chromate, which (because of its color) was maintained at 0.5 mM. When the inorganic substrate was varied, MgATP was present at 2.5 mM. $V_{max,app}$ values were determined from v vs [oxyanion] curves.

Equilibrium Constant. The K_{eq} of the APS synthesis reaction is related to the kinetic constants by the Haldane equation:

$$K_{eq} = \frac{V_{max,f}K_{iq}K_{mP}}{V_{max,r}K_{ia}K_{mB}} \quad (10)$$

The calculated value is about 1.6×10^{-7}, in good agreement with the value calculated for the enzyme from other sources (*23*, *27*, *41*, *50*, *24*).

Molybdolysis Activity. Molybdate has proven to be a useful alternative inorganic substrate for ATP sulfurylases (*51*). The advantage of molybdate over sulfate is that the APMo complex either never forms or decomposes almost instantly, regenerating MoO_4^{2-} along with coproducts PP_i and AMP. This changes a reaction with a normally very small equilibrium constant into an irreversible reaction and one that is not significantly inhibited by the accumulated PP_i (because there is no significant level of APMo in the steady state to which $MgPP_i$ could bind). The constants for the molybdolysis reaction catalyzed by human PAPSS1 are included in Table 1. Like other ATP sulfurylases that have been tested (including that from rat liver), the V_{max} with molybdate as the inorganic substrate is much greater than that with sulfate. But unlike other ATP sulfurylases, the E·MoO_4^{2-} dissociation constant (K_{ib}) and the Michaelis constant for molybdate (K_{mB}) are both about an order of magnitude larger than those for sulfate.

Action of Other Oxyanions. Several major environmental pollutants, including arsenate, selenate, chromate ("chromium VI"), tungstate, chlorate, and perchlorate, interact with ATP sulfurylase. The first four, which are divalent oxyanions, serve as alternative substrates that can be coupled to myokinase (Table 3), indicating that, like molybdate (*51*, *26*), they promote the hydrolysis of MgATP to AMP and PP_i. Selenate, chromate, and arsenate produce a sulfurylase product with a lifetime long enough to be captured and 3′-phosphorylated by APS kinase. Among the divalent substrates, chromate, a product of the electroplating, leather tanning, and wood preservation industries (*52*), is the most effective, having the highest $V_{max,app}/K_{mB,app}$ values—58 and 84, compared to 18 or less for the other divalent oxyanions. The accumulation of PAP in the assay medium confirmed that chromate, selenate, and (probably) arsenate formed 3′-phosphonucleotide products, albeit unstable ones. For example, after a 20 min incubation at 2.5 mM MgATP and K_m levels of oxyanion, 143 μM PAP was produced when chromate was the inorganic substrate. Selenate and arsenate produced 11 μM and 2 μM PAP, respectively. It is generally believed that the reduction products of chromate (*53*, *54*) are major toxic agents. Perhaps the depletion of ATP and the inhibition of PAPS formation by chromate may also contribute to its action. Arsenate is not very effective as a substrate but might be highly toxic if the putative APAs or PAPAs are reduced to arsenite (*55*) in vivo. Phosphate is the least effective substrate[2] but might cause problems if used as a buffer at high concentration (*23*).

Thiosulfate (SSO_3^{2-}), an unreactive sulfate analogue, was competitive with sulfate and noncompetitive with MgATP (data not shown), a dead-end inhibition pattern seen for ATP sulfurylases from several sources (*40*, *23*, *27*, *41*, *24*) and one that is consistent with the random binding of MgATP and sulfate.

Chlorate (used as a bleaching agent in the textile and paper industries) and perchlorate (used as a solid oxidant in explosives and missile propulsion systems) are the most potent monovalent oxyanion inhibitors of PAPSS1. At 2.5 mM MgATP and 0.4 mM sulfate, the $[I]_{0.5}$ values were 0.11 mM and 0.53 mM for chlorate and perchlorate, respectively. Micromolar levels of perchlorate inhibit iodine uptake by thyroid gland, and that is almost certainly its major mode of toxicity (*56*−*58*). But an additional long-term effect on ATP sulfurylase cannot be discounted. As observed for ATP sulfurylases from a variety of other sources (*47*, *23*, *27*, *41*, *24*), chlorate was competitive with sulfate and uncompetitive[3] with MgATP (data not shown). The limiting inhibition constant (determined from slope and intercept replots of the primary double-reciprocal plots (*29*, *24*) and the known K_{ia}/[A] and [B]/K_{mB} values) was 14 μM. This constant represents the chlorate dissociation constant from the ternary E·MgATP·ClO_3^- complex. Planar monovalent oxyanions (which also include fluorosulfonate and nitrate) probably bind to same three residues of the sulfate subsite that hold three of the outer oxygens of sulfate (*13*).

[2] A sulfate contamination level of 0.7% (w/w) in the K_2HPO_4 and NaH_2PO_4 used could account for the apparent activity with phosphate as the substrate, although the manufacturer states that these products contain a maximum of 0.003−0.005% sulfate.

[3] Uncompetitive inhibition against substrate A by an inhibitor competitive with substrate B is generally considered to indicate a compulsory ordered sequence (A binds before B). But this diagnosis is valid only if the inhibitor and the competitive substrate have about the same relative selectivities for the free E and EA species. In this respect, thiosulfate is a good mimic of sulfate. But monovalent oxyanions (at the concentrations used in our inhibition experiments) seem to bind almost exclusively to the binary E·MgATP complex.

Effect of Phenylalanine. Hommes and co-workers (*59*−*61*) suggested that inhibition of PAPS synthesis in brain by phenylalanine results in a deficiency of acidic sulfatides, rendering myelin basic protein vulnerable to proteolytic degradation, and that this may be a possible contributor to developmental problems in individuals afflicted with phenylketonuria. However, at K_m levels of substrates, the ATP sulfurylase activity of PAPSS1 (assayed in the absence or in the presence of added APS kinase) was unaffected by phenylalanine at concentrations up to 2 mM.

DISCUSSION

Isoform 1 of human bifunctional PAPS synthetase (the predominant form in brain) was expressed in *E. coli* and purified to near-homogeneity, and the component reactions were kinetically characterized. The enzyme was modestly activated by DTT. But upon consideration of the known structures of APS kinases and ATP sulfurylases from other organisms, PAPSS1 is not likely to require an essential Cys residue for substrate binding or catalysis. DTT probably acted by reducing disulfide linkages that formed accidentally during purification and storage. The fact that DTT did not inactivate the enzyme suggests that there are no essential disulfide linkages.

Earlier laboratory studies on PAPSS acting in the physiological direction were based on the overall rate of PAPS formation at known levels of MgATP and SO_4^{2-} (*62*−*65*, *22*, *45*). That assay would yield kinetics amenable to analysis by conventional means only if at least one of the following conditions is met: (a) the APS kinase activity is in great excess over the ATP sulfurylase activity, so that the latter is completely rate-limiting, or (b) APS produced by the ATP sulfurylase domain is transferred directly to the APS kinase site without being released into solution (i.e., APS is perfectly channeled). If condition a holds, the requirements for a valid coupled assay would be met and the kinetic constants obtained would correspond to those of the ATP sulfurylase domain acting in the APS synthesis direction. However, we have shown that the overall PAPS synthesis reaction rate is greatly accelerated by the addition of exogenous APS kinase, indicating that the endogenous APS kinase activity is not sufficient to keep pace with the sulfurylase activity. Because of this activity imbalance, PAPS synthesis rates assayed in the absence of added APS kinase will not depend in a systematic and predictable way on the known concentrations of added MgATP and sulfate but rather on an unknown and ever-changing concentration of the accumulating (and inhibitory) APS intermediate.

There is a limiting case where the observed overall reaction rate would have a fixed relationship to the concentrations of added MgATP and sulfate without APS kinase being in great excess over ATP sulfurylase. That is, if the ATP sulfurylase reaction attained chemical equilibrium very rapidly and equilibrium was maintained throughout the assay period. In this case, the concentration of accumulated APS would be "buffered" at a level related to the K_{eq} of the ATP sulfurylase reaction. Rapid equilibration is a possibility for human PAPSS1, when it is considered that the K_{eq} of the ATP sulfurylase reactions is very small (1.6×10^{-7} under standard assay conditions). Figure 5A (solid line) shows the theoretical v vs [MgATP] plot that would be obtained at 4 mM sulfate. The plot has the same shape as that for negative cooperativity ($n_H = 0.5$) or for multiple enzymes catalyzing the same reaction but has nothing to do with either phenomenon. The Hill coefficient of 0.5 is just a consequence of the square root relationship between the plotted variable, [MgATP], and the $[APS]_{eq}$, upon which the observed velocity depends. The data fit the Michaelis−Menten equation rather poorly, but with normal experimental error, the fit may appear acceptable. Over a narrow range of substrate concentration, the double-reciprocal plot (Figure 5B) may appear to be linear and a curve fit would return reasonable kinetic constants [$V_{max} = 0.03$ μmol min^{-1} (mg of protein)$^{-1}$; $K_{mA} = 0.2$ mM]. But these "constants" are not meaningfully related to the true kinetic constants of the ATP sulfurylase or APS kinase domains except by coincidence. For a true sulfurylase equilibrium to be established, PP_iase would have to be absent. If a trace level of PP_iase was present, the velocity curve would probably be intermediate between that

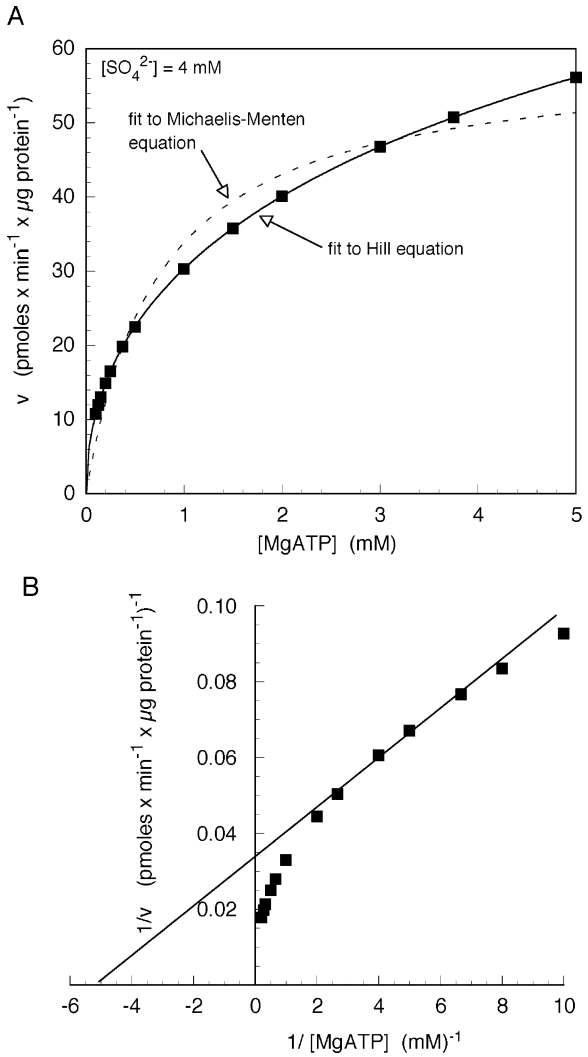

FIGURE 5: Simulated velocity curve for the synthesis of PAPS by human PAPSS1 with the assumption of rapid equilibration of the ATP sulfurylase step. Rates were calculated from eq 1 and the kinetic constants of the APS kinase domain (Table 1) along with the equilibrium level of APS that would be present at 4 mM sulfate and the indicated [ATP] as given by eq 5. K_{eq} of the ATP sulfurylase reaction was taken as 1.6×10^{-7}. (A) v vs [MgATP]. The line was fitted to the Michaelis−Menten equation (eq 2; broken line) and the Hill equation (eq 6; solid line). (B) Corresponding double-reciprocal plot of the data shown in panel A. The straight line was fitted visually.

shown in Figure 5A ($n_H = 0.5$) and a true hyperbola ($n_H = 1.0$) and the V_{max} would be a little higher.

If condition b holds—and APS channeling by PAPSS has been reported (*20*, *22*)—the overall activity might follow a recognized terreactant mechanism, e.g., a sequence where MgATP and sulfate add to the enzyme; catalysis occurs and $MgPP_i$ is released; APS moves to the kinase site where another molecule of MgATP adds and reacts; and finally, MgADP and PAPS are released. But APS channeling is, at best, imperfect. After all, exogenous APS can be bound by the ATP sulfurylase domain of PAPSS and converted to MgATP and sulfate in the reverse reaction. Exogenous APS can also bind to the APS kinase site. If APS can find its way from solution to the active sites, then it can also dissociate from those sites. The rate stimulation by added APS kinase (even at low substrate levels) confirms that efficient channeling does not occur. And the spectrophotometer tracings shown in Figure 3 confirm that APS dissociates from the enzyme and accumulates in solution. A report that unlabeled APS had no effect on the rate of ^{35}S incorporated into PAPS from subsaturating $^{35}SO_4^{2-}$ was taken as evidence for channeling (*22*). But adding unlabeled APS to an assay mixture in which labeled PAPS is being produced from $^{35}SO_4^{2-}$ would not yield a significant decrease in the rate of label conversion unless the resulting level of the free APS intermediate was well above its K_m for APS kinase. [The specific radioactivity of the intermediate would decrease upon addition of unlabeled APS, but the absolute rate might increase in a near-compensatory manner. A better approach would be to isolate and compare the specific radioactivity, i.e., counts per minute (cpm) per micromole, of the PAPS with that of the original $^{35}SO_4^2$.]

The *E. coli*-expressed, dimeric and His-tagged PAPSS1 described in this present report yielded normal (hyperbolic) initial velocity kinetics for MgATP and sulfate in the presence of excess exogenous APS kinase and PP_iase. In contrast, PAPSS1 expressed in COS-1 cells and assayed in the absence of added APS kinase has been reported to exhibit biphasic v vs $[SO_4^{2-}]$ kinetics (as in Figure 5B) and sigmoidal v vs [MgATP] kinetics, the latter with an n_H value of 5.5 (*45*). It remains to be determined whether these differences are a result of an actual difference between the enzyme expressed in different systems (e.g., perhaps there is a posttranslational enzyme modification in the mammalian cell system, or maybe the presence of the His tag in the *E. coli* expression system changed the kinetics) or whether the nature of the assays employed are responsible.

REFERENCES

1. Klaassen, C. D., and Boles, J. W. (1997) Sulfation and sulfotransferases 5: the importance of 3′-phosphoadenosine 5′-phosphosulfate (PAPS) in the regulation of sulfation, *FASEB J. 11*, 404−418.
2. Perrimon, N., and Bernfield, M. (2000) Specificities of heparan sulphate proteoglycans in developmental processes, *Nature 404*, 725−728.
3. Strott, C. A. (2002) Sulfonation and molecular action, *Endocr. Rev. 23*, 703−732.
4. Farzan, M., Mirzabekov, T., Kolchinsky, P., Wyatt, R., Cayabyab, M., Gerard, N. P., Gerard, C., Sodroski, J., and Choe, H. (1999) Tyrosine sulfation of the amino terminus of CCR5 facilitates HIV-1 entry, *Cell 96*, 667−676.
5. Choe, H., Li, W., Wright, P. L., Vasileva, N., Venturi, M., ..., and Farzan, M. (2003) Tyrosine sulfation of human antibodies contributes to recognition of the CCR5 binding region of HIV-1 gp120, *Cell 114*, 161−170.
6. Chen, L., and Segel, I. H. (1985) Purification and characterization of bile salt sulfotransferase from human liver, *Arch. Biochem. Biophys. 241*, 371−379.
7. Chou, H. C., Ozawa, S., Fu, P. P., Lang, N. P., and Kadlubar, F. F. (1998) Metabolic Activation of Methyl-Hydroxylated Derivatives of 7,12-Dimethylbenz[*a*]Anthracene by Human Liver Dehydroepiandrosterone-Steroid Sulfotransferase, *Carcinogenesis 19*, 1071−1076.
8. Geller, D. H., Henry, J. G., Belch, J., and Schwartz, N. B. (1987) Co-purification and characterization of ATP-sulfurylase and adenosine-5′-phosphosulfate kinase from rat chondrosarcoma, *J. Biol. Chem. 262*, 7374−7383.
9. Lyle, S., Stanczak, J., Ng, K., and Schwartz, N. B. (1994) Rat chondrosarcoma ATP sulfurylase and adenosine 5′-phosphosulfate kinase reside on a single bifunctional protein, *Biochemistry 33*, 5920−5925.
10. Rosenthal, E. T., and Leustec, T. (1995) A multifunctional protein in *Urechis caupo* has both ATP sulfurylase and APS kinase activity, *Gene 165*, 243−248.
11. MacRae, I. J., Segel, I. H., and Fisher, A. J. (2000) Crystal structure of adenosine 5′-phosphosulfate (APS) kinase from *Penicillium chrysogenum*, *Biochemistry 39*, 1613−1621.
12. Lansdon, E. B., Segel, I. H., and Fisher, A. J. (2002) Ligand-induced structural changes in Adenosine 5′-phosphosulfate (APS) kinase from *Penicillium chrysogenum*, *Biochemistry 41*, 13672−13680.
13. MacRae, I. J., Segel, I. H., and Fisher, A. J. (2001) Crystal structure of ATP sulfurylase from *Penicillium chrysogenum:* Insights into the allosteric regulation of sulfate assimilation, *Biochemistry 40*, 6795−6804.
14. Ullrich, T. C., Blaesse, M., and Huber, R. (2001) Crystal structure of ATP sulfurylase from *Saccharomyces cerevisiae*, a key enzyme in sulfate activation, *EMBO J. 20*, 316−329.
15. Ullrich, T. C., and Huber, R. (2001) The complex structures of ATP sulfurylase with thiosulfate, ADP, and chlorate reveal new insights in inhibitory effects and the catalytic cycle, *J. Mol. Biol. 313*, 1117−1125.
16. MacRae, I. J., Segel, I. H., and Fisher, A. J. (2002) Allosteric inhibition of ATP sulfurylase from *P. chrysogenum* by R state destabilization, *Nat. Struct. Biol. 9*, 945−949.
17. Besset, S., Vincourt, J. B., Amalric, F., and Girard, J. P. (2000) Nuclear localization of PAPS synthetase 1: a sulfate activation pathway in the nucleus of eukaryotic cells, *FASEB J. 14*, 345−54.
18. ul Haque, M. F., King, L. M., Krakow, D., Cantor, R. M., Rusiniak, M. E., Swank, R. T., Superti-Furga, A., Haque, S., Abbas, H., Ahmad, W., et al. (1998) Mutations in orthologous genes in human spondyloepimetaphyseal dysplasia and the brachymorphic mouse, *Nat. Genet. 20*, 157−162.
19. Kurima, K., Warman, M. L., Krishnan, S., Domowicz, M., Krueger, R. C., Jr., Deyrup, A., and Schwartz, N. B. (1998) A member of a family of sulfate-activating enzymes causes murine brachymorphism, *Proc. Natl. Acad. Sci. U.S.A. 95*, 8681−8685 [erratum: (1998) *Proc. Natl. Acad. Sci. U.S.A. 95*, 12071].
20. Lyle, S., Ozeran, J. D., Stanczak, J., Westley, J., and Schwartz, N. B. (1994) Intermediate channeling between ATP sulfurylase and adenosine 5′-phosphosulfate kinase from rat chondrosarcoma, *Biochemistry 33*, 6822−6827.
21. Lyle, S., Stanczak, J. D., Westley, J., and Schwartz, N. B. (1995) Sulfate-activating enzymes in normal and brachyomorphic mice: Evidence for a channeling defect, *Biochemistry 34*, 940−945.
22. Fuda, H., Shimizu, C., Lee, Y. C., Akita, H., and Strott, C. A. (2002) Characterization and expression of human bifunctional 3′-phosphoadenosine 5′-phosphosulphate synthase isoforms, *Biochem. J. 365*, 497−504.
23. Yu, M., Martin, R. L., Jain, S., Chen, L. J., and Segel, I. H. (1989) Rat Liver ATP−Sulfurylase: Purification, Kinetic Characterization, and Interaction with Arsenate, Selenate, Phosphate, and Other Inorganic Oxyanions, *Arch. Biochem. Biophys. 269*, 156−174.
24. Hanna, E., MacRae, I. J., Medina, D. C., Fisher, A. J., and Segel, I. H. (2002) ATP sulfurylase from the hyperthermophilic chemolithotroph *Aquifex aeolicus*, *Arch. Biochem. Biophys. 406*, 275−288.
25. MacRae, I., Rose, A. B., and Segel, I. H. (1998) Adenosine 5′-Phosphosulfate (APS) Kinase from *Penicillium chrysogenum*: Site Directed Mutagenesis at Putative Phosphoryl-Accepting and ATP P-loop Residues, *J. Biol. Chem. 273*, 28583−28589.

26. Segel, I. H., Renosto, F., and Seubert, P. A. (1987) in *Methods in Enzymology* (Jakoby, W. B., and Griffith, O. W., Eds.) pp 334−349, Academic Press, San Diego, CA.
27. Renosto, F., Martin, R. L., Borrell, J. L., Nelson, D. C., and Segel, I. H. (1991) ATP Sulfurylase from Trophosome Tissue of *Riftia pachyptila* (Hydrothermal Vent Tube Worm), *Arch. Biochem. Biophys. 290*, 66−78.
28. MacRae, I. J., and Segel, I. H. (1999) Adenosine 5′-phosphosulfate (APS) kinase: Diagnosing the mechanism of substrate inhibition, *Arch. Biochem. Biophys. 361*, 277−282.
29. Segel, I. H. (1993) *Enzyme Kinetics: Behavior and Analysis of Rapid Equilibrium and Steady-State Enzyme Systems*, Wiley-Interscience, New York.
30. Satishchandran, C., and Markham, G. D. (2000) Mechanistic studies of *Escherichia coli* adenosine-5′-phosphosulfate kinase, *Arch. Biochem. Biophys. 378*, 210−215.
31. Lillig, C. H., Schiffmann, S., Berndt, C., Berken, A., Tischka, R., and Schwenn, J. D. (2001) Molecular and catalytic properties of *Arabidopsis thaliana* adenylyl sulfate (APS)-kinase, *Arch. Biochem. Biophys. 392*, 303−10.
32. Venkatachalam, K. V., Akita, H., and Strott, C. A. (1998) Molecular cloning, expression, and characterization of human bifunctional 3′-phosphoadenosine 5′-phosphosulfate synthase and its functional domains, *J. Biol. Chem. 273*, 19311−19320.
33. Lowry, O. H., Passonneau, J. V., Hasselberger, F. X., and Schulz, D. W. (1964) Effect of Ischemia on known substrates and cofactors of the glycolytic pathway in brain, *J. Biol. Chem. 239*, 18−30.
34. Hems, D. H., and Brosnan, J. T. (1970) Effects of Ischaemia on the content of metabolites in rat liver and kidney in vivo, *Biochem. J. 120*, 105−111.
35. Greenbaum, A. L., Gumaa, K. A., and McLean, P. (1971) The distribution of hepatic metabolites and the control of the pathways of carbohydrate metabolism in animals of different dietary and hormonal status, *Arch. Biochem. Biophys. 143*, 617−663.
36. Veech, R. L., Lawson, J. W. R., Cornell, N. W., and Krebs, H. A. (1979) Cytosolic phosphorylation potential, *J. Biol. Chem. 254*, 6538−6547.
37. Cole, D. E., and Scriver, C. R. (1980) Age-dependent serum sulfate levels in children and adolescents, *Clin. Chem. Acta 107*, 135−139.
38. Krijgsheld, K. R., and Mulder, G. J. (1982) The availability of inorganic sulfate as a rate-limiting factor in the sulfation of xenobiotics in mammals in vivo, in *Sulfate Metabolism and Sulfate Conjugation* (Mulder, G. J., Caldwell, J., Van Kempen, G. M. J., and Vonk, R. J., Eds.) pp 59−66, Taylor and Francis, London.
39. Morris, M. E., and Levy, G. (1983) Serum concentration and renal excretion by normal adults of inorganic sulfate after acetaminophen, ascorbic acid, or sodium sulfate administration, *Clin. Pharmocol. Ther. 33*, 529−536.
40. Seubert, P., Renosto, F., Knudson, P., and Segel, I. H. (1985) Adenosinetriphosphate sulfurylase from *Penicillium chrysogenum:* Steady-state kinetics of the forward and reverse reactions, alternative substrate kinetics and equilibrium binding studies, *Arch. Biochem. Biophys. 240*, 509−523.
41. Renosto, F., Patel, H. C., Martin, R. L., Thomassian, C., Zimmerman, G., and Segel, I. H. (1993) ATP Sulfurylase from Higher Plants: Kinetic and Structural Characterization of the Chloroplast and Cytosol Enzymes from Spinach Leaf, *Arch. Biochem. Biophys. 307*, 272−285.
42. Hanna, E., Ng, K. F., MacRae, I. J., Bley, C. J., Fisher, A. J., and Segel, I. H. (2004) Kinetic and stability properties of *Penicillium chrysogenum* ATP sulfurylase missing the C-terminal regulatory domain, *J. Biol. Chem. 279*, 4415−4424.
43. Xu, Z., Wood, T. C., Adjei, A. A., and Weinshilboum, R. M. (2001) Human 3′-phosphoadenosine 5′-phosphosulfate synthetase: radiochemical enzymatic assay, biochemical properties, and hepatic variation, *Drug Metab. Dispos. 29*, 172−8.
44. Xu, Z. H., Freimuth, R. R., Eckloff, B., Wieben, E., and Weinshilboum, R. M. (2002) Human 3′-phosphoadenosine 5′-phosphosulfate synthetase 2 (PAPSS2) pharmacogenetics: gene resequencing, genetic polymorphisms and functional characterization of variant allozymes, *Pharmacogenetics 12*, 11−21.
45. Xu, Z.-H., Thomae, B. A., Eckloff, B. W., Weiben, E. D., and Weinshilboum, R. M. (2003) Pharmacogenetics of human 3′-phosphoadensoine 5′-phosphosulfate symntetase 1 (PAPSS1): gene resequencing, sequence variation, and functional genomics, *Biochem. Pharmacol. 65*, 1787−1796.
46. Daley, L. A., Renosto, F., and Segel, I. H. (1986) ATP sulfurylase-dependent assays for inorganic pyrophosphatase: Applications to determining the equilibrium constant and reverse direction kinetics of the pyrophosphatase reaction, magnesium binding to orthophosphate, and unknown concentrations of pyrophosphate, *Anal. Biochem. 157*, 385−395.
47. Seubert, P. A., Hoang, L., Renosto, F., and Segel, I. H. (1983) ATP Sulfurylase from *Penicillium chrysogenum*: Measurements of the True Specific Activity of an Enzyme Subject to Potent Product Inhibition and a Reassessment of the Kinetic Mechanism, *Arch. Biochem. Biophys. 225*, 679−691.
48. Renosto, F., Seubert, P. A., and Segel, I. H. (1984) Adenosine-5′-Phosphosulfate Kinase from *Penicillium chrysogenum*: Purification and Kinetic Characterization, *J. Biol. Chem. 259*, 2113−2123.
49. Singh, B., and Schwartz, N. B. (2003) Identification and Functional Characterization of the Novel BM-motif in the Murine Phosphoadenosine Phosphosulfate (PAPS) Synthetase, *J. Biol. Chem. 278*, 71−5.
50. Foster, B. A., Thomas, S. M., Mahr, J. A., Renosto, F., Patel, H., and Segel, I. H. (1994) Cloning and sequencing of ATP sulfurylase from *Penicillium chrysogenum*: Identification of a likely allosteric domain, *J. Biol. Chem. 269*, 19777−19786.
51. Wilson, L. G., and Bandurski, R. S. (1958) Enzymatic Reactions Involving Sulfate, Sulfite, Selenate, and Molybdate, *J. Biol. Chem. 233*, 975−981.
52. Ellis, A. S., Johnson, T. M., and Bullen, T. D. (2002) Chromium isotopes and the fate of hexavalent chromium in the environment, *Science 295*, 2060−2062.
53. Wetterhahn, K. E., and Hamilton, J. W. (1989) Molecular basis of hexavalent chromium carcinogenicity: Effect on gene expression, *Sci. Total Environ. 86*, 113−129.
54. Kortenkamp, A., Casadevall, M., Faux, S. P., Jenner, A., Shayer, R. O. J., Woodbridge, N., and Obrien, P. (1996) A Role for Molecular Oxygen in the Formation of DNA Damage During the Reduction of the Carcinogen Chromium(VI) by Glutathione, *Arch. Biochem. Biophys. 329*, 199−207.
55. Knowles, F. (1986) Enzymatic reactions involving orthoarsenate: arsenate is competitive with sulfate in the ATP sulfurylase reaction, *Arch. Biochem. Biophys. 251*.
56. Greer, M. A., Goodman, G., Pleus, R. C., and Greer, S. E. (2002) Health effects assessment for environmental perchlorate contamination: The dose response for inhibition of thyroidal radioiodine uptake in humans, *Environ. Health Perspect. 110*, 927−937.
57. Urbansky, E. T. (2002) Perchlorate as an environmental contaminant, *Environ. Sci. Pollut. Res. 9*, 187−192 (review).
58. Mahle, D. A., Yu, K. O., Narayanan, L., Mattie, D. R., and Fisher, J. W. (2003) Changes in cross-fostered Sprague-Dawley rat litters exposed to perchlorate, *Int. J. Toxicol. 22*, 87−94.
59. Hommes, F. A. (1985) Myelin turnover at later stages of brain development in experimental hyperphenylalaninemia, in *Inherited Diseases of Amino Acid Metabolism: Recent progress in the understanding, recognition and management*, International Symposium in Heidelberg (Bickel, H., and Wachtel, U., Eds.) pp 64−85, Thieme, Stuttgart, Germany.
60. Hommes, F. A. (1985) Amino acidaemias and brain maturation: interference with sulphate activation and myelin metabolism, *J. Inher. Metab. Dis. 8*, 121−122.
61. Matsuo, K., Moss, L., and Hommes, F. A. (1987) In vivo and in vitro tyrosine sulfation of a membrane glycoprotein, *Neurochem. Res. 12*, 345−349.
62. Deyrup, A. T., Krishnan, S., Singh, B., and Schwartz, N. B. (1999) Activity and stability of recombinant bifunctional rearranged and monofunctional domains ATP sulfurylase and adenosine 5′-phosphosulfate kinase, *J. Biol. Chem. 274*, 10751−10757.
63. Deyrup, A. T., Singh, B., Krishnan, S., Lyle, S., and Schwartz, N. B. (1999) Chemical modification and site-directed mutagenesis of conserved HXXH and PP-loop motif arginines and histidines in murine bifunctional ATP sulfurylase/adenosine 5′-phosphosulfate kinase, *J. Biol. Chem. 274*, 28929−28936.
64. Venkatachalam, K. V., Fuda, H., Koonin, E. V., and Strott, C. A. (1999) Site-directed mutagenesis of a conserved nucleotide binding HXGH motif located in the ATP sulfurylase domain of human bifunctional 3′-phosphoadenosine 5′-phosphosulfate synthase, *J. Biol. Chem. 274*, 2601−2604.
65. Venkatachalam, K. V. (2003) Human 3′-phosphoadenosine 5′-phosphosulfate (PAPS) synthase: Biochemistry, molecular biology and genetic deficiency, *IUBMB Life 55*, 1−11 (review).

BI049827M